

A Similarity Analysis of the Droplet Trajectory Equation

Michael B. Bragg*

Ohio State University, Columbus, Ohio

A procedure is established to reduce the number of similarity parameters in the trajectory equation for particles in a moving fluid. This is accomplished by the use of an approximate sphere drag law to derive a new trajectory scaling parameter. The modified inertia parameter proposed by Langmuir specifically for the aircraft icing problem is analyzed and for the first time a closed-form solution is obtained. Both experimental and analytical results are presented to verify this new trajectory scaling parameter.

Nomenclature

C	= proportionality constant in approximate drag law
c	= characteristic length, m
C_D	= droplet drag coefficient, $D/(\frac{1}{2}\rho U^2 S)$
D	= droplet drag, N
E	= total droplet collection efficiency
F_r	= Froude number, U/\sqrt{cg}
g_0	= gravitational constant, m/s ²
\vec{g}	= gravitational acceleration vector, m/s ²
K	= inertia parameter, $\sigma\delta^2 U/18c\mu$
K_0	= modified inertia parameter, $K(\lambda/\lambda_s)$
\bar{K}	= trajectory scaling parameter, K/R_U^2
m	= mass of droplet, kg
R	= droplet relative Reynolds number, $\rho\delta U \vec{u} - \dot{\vec{\eta}} /\mu$
R_U	= droplet freestream Reynolds number, $\rho\delta U/\mu$
S	= droplet cross-sectional area, m ²
t	= time, s
U	= freestream velocity, m/s
\vec{u}	= flowfield velocity vector, dimensionless with U
\vec{x}	= droplet position vector, m
β	= exponent in approximate drag law and \bar{K}
δ	= droplet diameter, m
$\vec{\eta}$	= dimensionless droplet position vector, \vec{x}/c
λ/λ_s	= droplet trajectory ratio, Eq. (6)
ρ	= air density, kg/m ³
σ	= droplet density, kg/m ³
τ	= dimensionless time, Ut/c
μ	= absolute air viscosity, kg/m-s
$()_m$	= scale model value

I. Introduction

THE calculation of the trajectories of small spherical droplets in a moving fluid finds applications in many areas of science and engineering. These include propulsion problems, several topics in atmospheric sciences, the application of agricultural chemicals, and aircraft icing to name only a few. As in other areas of engineering, the derivation of the similarity parameters governing the problem greatly simplifies the analysis. Two particular applications of the similarity parameters are of interest here.

The first application is to facilitate the collection and presentation of experimental or numerical data. The droplet trajectories will be shown under certain conditions to be a function of a single dimensionless parameter, which simplifies the analysis considerably. The second use of the parameter will be to serve as a scaling parameter for model testing. The reduction of the similarity parameters governing the problem to a single nondimensional number makes model testing

feasible in situations which could not be scaled properly before.^{1,2}

First, the complete set of similarity parameters will be derived from the differential equation. Earlier attempts to simplify the scaling analysis will be discussed and the current method presented. Finally, the analysis will be demonstrated using both experimental and analytical results.

II. Theoretical Development

Trajectory Equation

By applying Newton's Second Law of Motion to a single spherical particle moving relative to the surrounding fluid, the differential equation describing the droplet trajectory can be derived. Although many forces act on the particle, for most applications only the viscous drag and the body force due to gravity need be considered. Including only these two force terms, the differential equation is

$$m \frac{d\vec{x}^2}{dt^2} = \vec{D} + m\vec{g} \quad (1)$$

where m is the droplet mass and \vec{x} the position vector. In nondimensional form the equation becomes

$$K\ddot{\vec{\eta}} = \left(\frac{C_D R}{24}\right)(\vec{u} - \dot{\vec{\eta}}) + \frac{K}{F_r^2} \left(\frac{\vec{g}}{g_0}\right) \quad (2)$$

Here $\vec{\eta}$ is the dimensionless position vector, \vec{u} the dimensionless flowfield velocity, and the dot represents the derivative with respect to nondimensional time τ . The dimensionless parameters which appear explicitly in Eq. (2) are K , the inertia parameter and F_r , the Froude number given by

$$K = \sigma\delta^2 U/18c\mu; \quad F_r = U/\sqrt{cg} \quad (3)$$

For many applications the sphere drag may be expressed as a function only of the relative Reynolds number, $R = R_U |\vec{u} - \dot{\vec{\eta}}|$. Then, from the Stokes law parameter, $C_D R/24$, comes the third similarity parameter R_U , the freestream Reynolds number based on droplet diameter,

$$R_U = \rho U \delta / \mu \quad (4)$$

This assumption of the functional form of the viscous drag term holds well into the compressible regime provided the Mach number based on droplet relative velocity is low.

Provided the preceding assumptions are not violated, a single particle trajectory is a function of only the droplet Reynolds number, Froude number, and inertia parameter. These parameters are cumbersome to use in presenting data. When used as scaling parameters, holding these dimensionless

Received Sept. 24, 1981; revision received Feb. 26, 1982. Copyright © American Institute of Aeronautics and Astronautics, Inc., 1982. All rights reserved.

*Assistant Professor, Dept. of Aeronautical and Astronautical Engineering. Member AIAA.

numbers constant often violates the flowfield scaling and leads to unattainable test conditions.

Simplified Parameters

The use of R_U , K , and F_r to establish model test conditions often leads to serious problems. Ormsbee and Bragg¹ used these parameters to scale the trajectory of drops in aircraft wakes. The resulting test particles were very large in diameter and low in density. The particles were difficult to obtain and for small-scale tests the densities required become so low as to violate assumptions made in the derivation of Eq. (2). When the particles are small and gravity can be ignored, only R_U and K must be held constant. This still leads to problems in cases such as aircraft icing model tests where only the model speed and droplet diameter are variables. Holding R_U and K constant requires that

$$\delta_m = (c_m/c)\delta \quad \text{and} \quad U_m = (c/c_m)U$$

For small-scale models the test velocity required is very large and violates the Mach number scaling of the flowfield.² Recent tests by a Soviet-Swedish research group³ chose to ignore the Reynolds number scaling and held only the inertia parameter constant in an attempt to avoid this problem.

Methods are available to avoid these problems by reducing the number of similarity parameters. First Langmuir's classical modified inertia parameter will be discussed and a new derivation presented. Then the present method will be derived and shown to be much simpler to use and in some cases more accurate.

Modified Inertia Parameter

The modified inertia parameter K_0 was presented by Langmuir in 1946⁴ to be used to present aircraft icing data. In fact, this parameter is still in wide use in the aircraft icing community although no theoretical proof of its validity is available.⁵ Currently, no closed-form solution for the parameter is available and a graphical technique or curve fit to the numerically generated data is used. Here the K_0 parameter will be discussed and a theoretical proof of its validity will be presented which yields a closed-form solution.

The modified inertia parameter K_0 is defined as

$$K_0 = K(\lambda/\lambda_s) \quad (5)$$

where K is the inertia parameter and λ/λ_s the ratio of the length of the trajectory of a droplet in still air, with an initial Reynolds number of R_U and gravity neglected, divided by the same trajectory of the droplet if the drag is assumed to obey Stokes law. So K_0 combines K and R_U into a single parameter since λ/λ_s is a function of R_U . Langmuir showed that λ/λ_s is given by

$$\lambda/\lambda_s = \frac{1}{R_U} \int_0^{R_U} \frac{dR}{(C_D R/24)} \quad (6)$$

Using the standard sphere drag curve for $C_D R/24$ Langmuir performed this integration numerically to generate λ/λ_s as a function of R_U which is still in use today.

By using the differential Eq. (2), the origin of Langmuir's K_0 parameter can be examined more carefully. It is not clear from Ref. 4 if Langmuir derived K_0 in this way, but the basic relationship between K_0 and the governing differential equation was presented in 1952 in Ref. 6.

In Eq. (2) by dropping the gravity term and rearranging we obtain

$$\left[\frac{K}{(C_D R/24)} \right] \ddot{\eta} = (\ddot{u} - \dot{\eta}) \quad (7)$$

Here $C_D R/24$ is a complex function of R with R varying along the particle trajectory. If some suitable average of the term on the left-hand side of Eq. (7) can be found, the R_U and K parameters can be combined into a single similarity parameter. Let us assume that the particle experiences Reynolds numbers from zero to R_U , the value based on the freestream velocity. Then, averaging this term yields

$$K_0 = \frac{K}{R_U} \int_0^{R_U} \frac{dR}{(C_D R/24)} \quad (8)$$

K_0 is merely the average value of the single coefficient which appears in the droplet trajectory Eq. (7). K_0 is not an exact similarity parameter, but does have valid theoretical justification as it is a straightforward simplification of the governing particle trajectory equation. The modified inertia parameter provides good data correlation provided the range of Reynolds numbers experienced by the particle is consistent with the range zero to R_U . This point will be discussed in more detail later.

A closed form expression for K_0 can be found if an integrable form of the droplet drag coefficient is used in Eq. (8). Putnam⁷ has developed such an equation valid up to a Reynolds number of 1000 as

$$C_D R/24 = 1 + (1/6)R^{3/2} \quad (9)$$

Following the work of Putnam, or by direct integration of Eq. (8) using Eq. (9) for $C_D R/24$, a closed form of K_0 is given as

$$K_0 = 18K \left[R_U^{-3/2} - \sqrt{6} R_U^{-1} \tan^{-1} \left(\frac{R_U^{1/2}}{\sqrt{6}} \right) \right] \quad (10)$$

This equation is within 2% of Langmuir's calculated values until R_U approaches 1000, where Langmuir's values deviate from those of Eq. (10), probably because of the loss of accuracy in the numerical procedure, and the applicable range of Eq. (9).

The lower limit of Eq. (10) can be used to check the derivation of K_0 . By definition K_0 must approach the inertia parameter for small values of the Reynolds number where the particle drag is essentially governed by Stokes law. By expanding the inverse tangent function and taking the limit as R_U approaches zero, Eq. (10) reduces as expected to $K_0 = K$. By examining Eq. (10) as R_U approaches infinity, K_0 takes the form

$$K_0 = 18KR_U^{-3/2} \quad (11)$$

It is also interesting to compare the curve fit developed by Lozowski et al.⁸ for K_0 where

$$K_0 = \frac{K}{1 + 0.0967 R_U^{0.6367}} \quad (12)$$

This also compares well to Eq. (10); note the similarity in the $1/R_U^{0.6367}$ term in Eq. (12) and the $R_U^{-3/2}$ expression in Eq. (10).

The use of Eq. (10) should improve the usefulness of the existing icing data correlated with K_0 . Eliminating interpolation or curve fits to Langmuir's tabulated data should also improve accuracy. Equation (10) could be used to reduce other droplet trajectory data, however, the analysis to follow will result in a parameter which is easier to use, more versatile, and provides better accuracy than K_0 in certain situations.

Present Method

An alternate approach can be taken to simplify the single coefficient appearing in the trajectory Eq. (7). Instead of

assuming an average value of $C_D R/24$, as was done to derive K_0 , here assume that

$$C_D R/24 = CR^\beta \quad (13)$$

which appears as a straight line on the log-log plot of $C_D R/24$ vs R . A similar approximation has been made before by Ormsbee and Bragg^{1,9} and by Armand et al.¹⁰ to scale droplet trajectories. The trajectory equation then becomes

$$\ddot{\eta} = C \left(\frac{R_U^\beta}{K} \right) |\bar{u} - \dot{\eta}|^\beta (\bar{u} - \dot{\eta}) \quad (14)$$

Now define the trajectory similarity parameter \bar{K} as

$$\bar{K} = K/R_U^\beta \quad (15)$$

where the term in Eq. (14) has been inverted to follow the convention established by the K_0 parameter.

The appearance of the $|\bar{u} - \dot{\eta}|^\beta$ term in Eq. (14) simplifies the use of this parameter. Since a β occurs outside the \bar{K} term, C and β cannot, in general, be functions of R_U , but must be chosen from a single best fit of $C_D R/24 = CR^\beta$ over the entire range of Reynolds numbers to be experienced by all particles under consideration. Then, after the constants C and β have been chosen for a particular application, the droplet trajectory equation, Eq. (14), is a function of \bar{K} only (for similar flowfields). A simple parameter combining K and R_U is now available to be used for data presentation or establishing scale-model test conditions. Note that if the gravity term need be included, this requires only that the Froude number F_r also be considered in addition to \bar{K} . In the next section both experimental and analytical data will be presented to verify \bar{K} along with some guidelines on the selection of β .

III. Results and Discussion

The use of the \bar{K} parameter to scale particle trajectories has been demonstrated by Ormsbee and Bragg¹ for spherical particles in aircraft wakes. A summary of those results will be presented here. Aircraft icing data on droplet trajectories will be used to compare the modified inertia parameter K_0 and the \bar{K} parameter to determine how they are related and the relative accuracy of each.

Experimental Verification

Recent published results by Ormsbee and Bragg¹ demonstrate the method and validity of the use of \bar{K} as a droplet trajectory scaling parameter. In these tests conducted in the NASA Langley vortex research facility three geometrically scaled agricultural aircraft models were used to inject scaled spherical particles into the model wake. Using the complete set of similarity parameters for the droplet dynamics R_U , K , and F_r results in a unique scaled test particle of low density and large diameter. Relaxing the constraints on the scaled particles by replacing R_U and K by \bar{K} yields an infinite number of candidate test particles greatly simplifying the task of particle selection.

Table 1 Physical variables

	Model scale			1.0
	0.10	0.15	0.20	
Wing semispan, m	1.22	1.83	2.44	40.0
Model velocity, m/s	16.8	20.6	23.8	53.3
Altitude, m	0.622	0.933	1.24	20.4
Angle of attack, deg	2.00	2.00	2.00	2.00
Particle diameter, μm	105.0	125.0	105.0	490.0
Particle density, g/cm ³	2.42	2.42	3.99	1.0

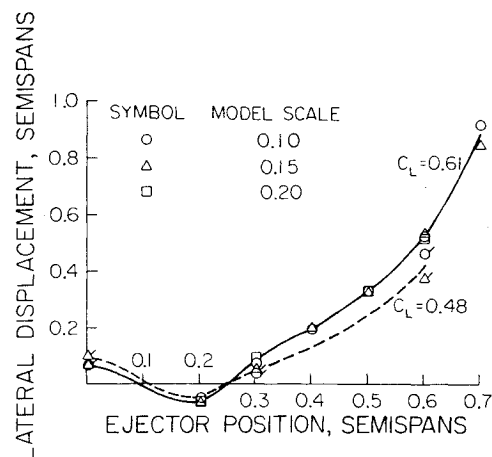


Fig. 1 Experimental results scaling droplet trajectories in an aircraft wake.

In these tests a hypothetical full-scale aircraft and droplet test conditions were chosen. These were then scaled to determine the equivalent test condition for 0.10, 0.15, and 0.20 scale models. Table 1 shows the full-scale and model test conditions while the particle trajectory results are summarized in Fig. 1. The particles were injected into the flow from containers in the wing at several spanwise locations. Presented in Fig. 1 is the lateral transport of the particles by the wake vortex system as a function of initial injector location. For all three models the lateral transport of the scaled particles is the same; thus verifying the \bar{K} scaling analysis. Scaling tests were also reported in Ref. 1 where other lift coefficients, aircraft altitudes, and full-scale droplet sizes were used and in all cases the particle trajectories scaled well.

Aircraft Icing Scaling

For the case of aircraft icing the droplets considered are in a range of 10-50 μm . Therefore, the gravity term is negligible compared to the viscous drag, and the Froude number may be dropped. This simplifies the analysis and permits the easy comparison of K_0 and \bar{K} since, in this case, the droplet trajectory becomes a function of only the one dimensionless number and the initial droplet condition for a given flowfield.

A careful analysis of the modified inertia parameter K_0 and the trajectory scaling parameter \bar{K} shows that the two parameters are closely related. If the approximate drag law of Eq. (13) is assumed and used in Eq. (8) the result is

$$K_0 = \frac{K}{C(1-\beta)R_U^\beta}$$

This is equivalent to approximating the λ/λ_s term in K_0 as proportional to R_U^β . This approximate K_0 expression has been used by the aircraft industry for icing scaling,¹¹ where β was determined from Langmuir's numerical λ/λ_s as a function of R_U data. For this special case, K_0 differs from \bar{K} by only a constant.

While the general form of K_0 given by Eq. (10) is more complicated, it too can be seen to be in a functional form similar to that of \bar{K} . Taking the limit of both K_0 and \bar{K} as R_U approaches zero yields just K in both instances. As R_U approaches infinity the limit of K_0 is $K_0 = 18KR_U^{-2/3}$ as given earlier in Eq. (11). This is exactly $\bar{K}/18$ if $\beta = 2/3$. Therefore, it has been shown that K_0 and \bar{K} have the same limits with respect to R_U within a constant. In addition, K_0 and \bar{K} are the same within a constant if a simple drag law is assumed in deriving K_0 .

A method for selecting the β to be used in the \bar{K} parameter must be determined. The selection of a β depends on the range of Reynolds numbers to be experienced by the particles during

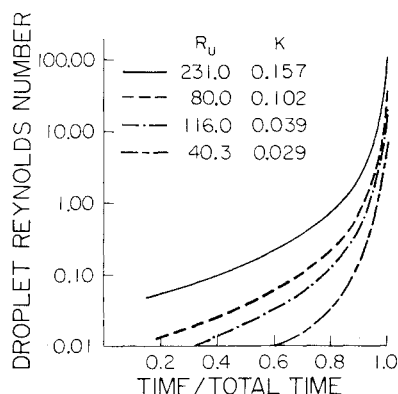


Fig. 2 Typical Reynolds number experienced during droplet trajectory.

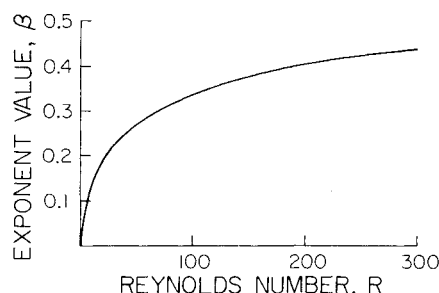


Fig. 3 Approximate drag law exponent for best fit in Reynolds number range 0-R.

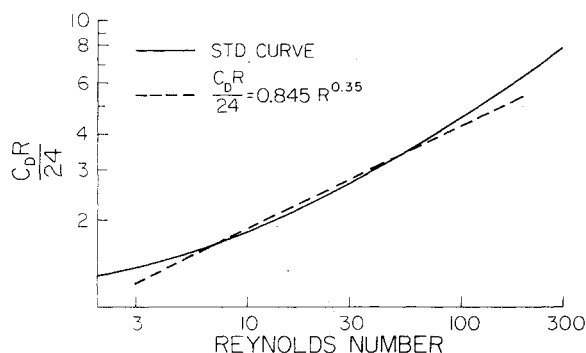


Fig. 4 Standard sphere drag curve and approximation.

their trajectories. Since a β term occurs in the differential equation outside the \bar{K} term [see Eq. (14)] only one β may be selected for each application of \bar{K} . For a scaling application a different β may be selected for each particle considered, however, when \bar{K} is used to present data, an average value of β which is good over all possible particle trajectories to be presented must be used.

It has been found that the particles injected into aircraft wakes experience Reynolds numbers slightly larger than their terminal values. So for this application β was determined by using a least squares analysis to find the β which provided the best fit to the standard sphere drag curve. The actual Reynolds number range was from the terminal Reynolds number of the scaled particle to twice the terminal Reynolds number of the full-scale particle. Using this scheme provided good results as seen in Fig. 1.

For the icing problem the Reynolds number range experienced by a particle is somewhat different. The supercooled water droplets are initially at rest with respect to the atmosphere and, therefore, the Reynolds number is zero. The maximum Reynolds number experienced by the droplet is when it is in the immediate proximity of the aircraft com-

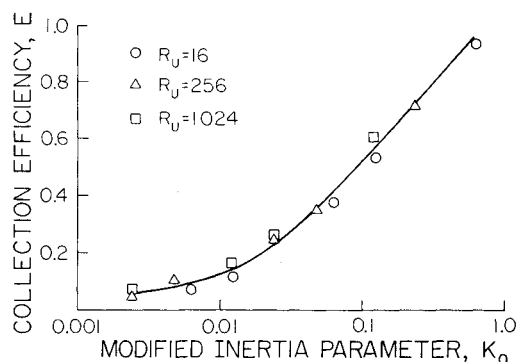


Fig. 5 Collection efficiency of an NACA 65A004 airfoil as a function of K_0 .

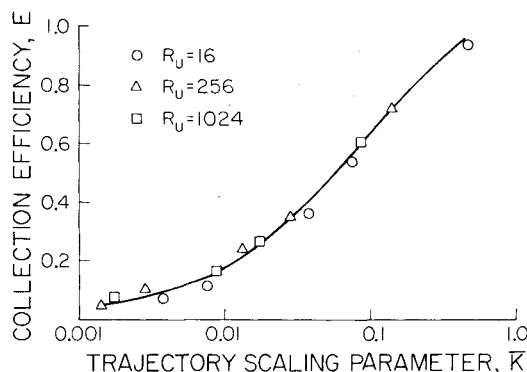


Fig. 6 Collection efficiency of an NACA 65A004 airfoil as a function of \bar{K} .

ponent where the velocity gradients are large, causing a significant relative velocity between the particle and the local fluid. In Fig. 2, the droplet Reynolds number is shown along the trajectory of four different droplets. This information was generated using the computer program of Ref. 2 for droplets starting five chord lengths in front of a typical general aviation airfoil section at a cruise condition. Note that the particles all experience Reynolds numbers in the Stokes law range for the first 80% of their trajectories. Only as the droplets approach the body do the Reynolds numbers increase drastically. However, for no case analyzed to date has the droplet Reynolds number ever reached the value based on the freestream velocity R_U . In fact, the droplets usually experience a maximum Reynolds number of less than $0.5R_U$.

Using this information on the typical Reynolds number range along with Fig. 3 a value of β can be determined. Figure 3 summarizes the results of a least squares fit program which calculates the value of β that provides the best fit of the approximate sphere drag expression of Eq. (13) to the standard sphere drag curve. The fit is performed from a Reynolds number of zero to R . Figure 4 shows the standard sphere drag curve and the approximate drag law, where for this example $\beta = 0.35$. It has been found that for the aircraft icing problem a β of 0.35 represents a good average value to be used for preliminary scaling calculation and for data presentation. To select a β to use in scaling a particular droplet, the average value of R_U for the full-scale and scaled particle is found and then Fig. 3 can be used to determine β . In general, this is an iterative procedure, but by using $\beta = 0.35$ to select the initial scaled R_U it converges quickly; usually the first step is sufficiently accurate.

Historically, icing data has been presented using the modified inertia parameter K_0 . The degree to which K_0 compresses this data to a single curve provides a measure of the accuracy of the approximation. Figure 5 shows the airfoil collection efficiency for three different freestream Reynolds numbers¹² plotted vs K_0 . The airfoil used was a NACA

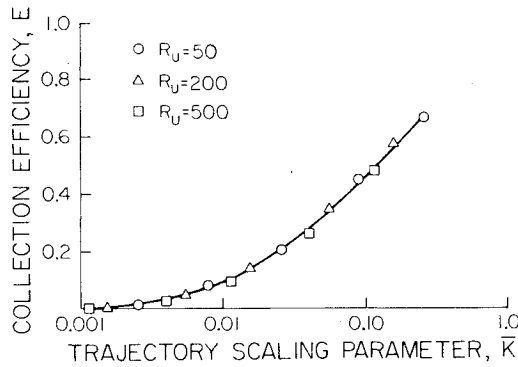


Fig. 7 Collection efficiency of an NACA 0012 airfoil as a function of \bar{K} .

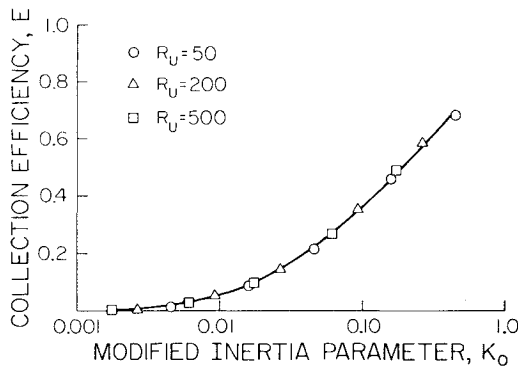


Fig. 8 Collection efficiency of an NACA 0012 airfoil as a function of K_0 .

65A004 and the droplet trajectories used to determine the collection efficiency were calculated numerically. The same data are plotted using \bar{K} in Fig. 6, where $\beta = 0.35$ as discussed earlier. Similar data on a NACA 0012 airfoil have been generated more recently using the computer code of Ref. 2. These results are shown in Figs. 7 and 8. Here again three values of R_U were used and K was varied from 0.01 and 1.0. Both parameters do an excellent job of reducing the data to a single curve, with neither method demonstrating improved accuracy over the other.

For scaling droplet trajectories the \bar{K} parameter has a definite edge over K_0 since β may be optimized for each droplet to be scaled. Figure 9 shows the local impingement efficiency plotted as a function of position on the airfoil leading edge for the full-scale and one-sixth scale model. The local impingement efficiency is the nondimensional mass flux of droplets striking the airfoil surface and is determined based on the trajectory calculations of several particles. The procedure for determining β described earlier yields a β of 0.30 for the 15- μm full-scale droplet and 0.39 for the 30- μm size droplet. The values of R_U and K used, as well as the droplet diameter δ , are given in Table 2. Note that for this example it was assumed that only the particle diameter would be changed to provide the trajectory scaling and that all other variables such as aircraft velocity, droplet density, air density,

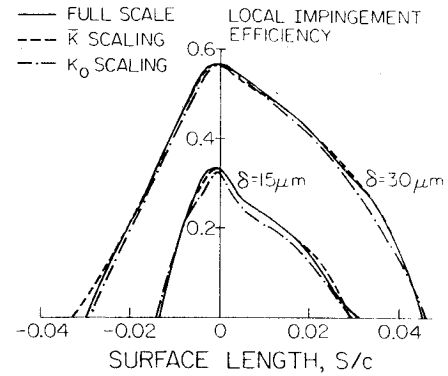


Fig. 9 Comparison of K_0 and \bar{K} in scaling the droplet impingement efficiency on an airfoil.

etc. would be held constant. This yields an equation for the scaled droplet diameter of

$$\delta_m = (c_m/c)^{1/(2-\beta)} \delta$$

The important results of the comparison in Fig. 9 are given in Table 3. Here E is the total collection efficiency and is proportional to the total mass of ice collected by the body. The maximum local collection efficiency governs the maximum growth rate of ice on the body. While K_0 does a reasonable job of reproducing the full-scale trajectories, the added flexibility in the \bar{K} parameter allows for an improved trajectory scaling.

IV. Summary and Conclusions

A systematic procedure has been presented to reduce the number of similarity parameters governing this class of particle trajectories. The method of Langmuir, that was previously little understood, has been derived from the governing differential equation and a closed-form solution was presented. This result should clarify the theoretical basis for the modified inertia parameter and make the existing data correlated using K_0 easier to interpret.

A new dimensionless number \bar{K} , the trajectory scaling parameter, was derived. This parameter is more accurate in some situations and more versatile than the modified inertia parameter. The trajectory scaling parameter may be used to simplify many trajectory analyses. \bar{K} simply combines R_U and K into a single dimensionless number to which dimensionless parameters from the other particle force terms such as the Froude number F_r may be added if needed. All that is required is the determination of the exponent β in the approximate drag law used in deriving \bar{K} . The exponent may be found by following the procedure.

1) Determine the range of Reynolds numbers experienced by the class of particles for which the \bar{K} parameter is to be used.

2) By using a least squares or other best fit scheme, determine the β for which the approximate drag law best fits the standard drag curve in the Reynolds number range of interest.

Table 2 Scaled variables

	Full scale	One-sixth scale model	
		\bar{K}	K_0
$\delta, \mu\text{m}$	15.0	5.23	5.05
R_U	115.6	40.30	38.93
K	0.0393	0.0286	0.0267
$\delta, \mu\text{m}$	30.0	9.86	9.60
R_U	231.2	75.97	73.98
K	0.1572	0.1018	0.0966

Table 3 Scaling comparison

	Full scale	One-sixth scale model	
		\bar{K}	K_0
$\delta = 15 \mu\text{m}$			
E	0.0555	0.0557	0.0508
Max local efficiency	0.332	0.331	0.323
$\delta = 30 \mu\text{m}$			
E	0.173	0.174	0.166
Max local efficiency	0.568	0.568	0.563

Experimental and numerical results have been presented in support of the \bar{K} parameter. These results for specific particle trajectory applications demonstrate the accuracy of the method. In addition, the trajectory scaling parameter is simple to use and results in accurate trajectory scaling and a great reduction in the work of data presentation.

The trajectory scaling parameter will work well in many situations, provided the appropriate Reynolds number range can be determined. The accuracy of the approximation will naturally improve as the range of Reynolds numbers experienced by the droplets decreases. By reducing the number of similarity parameters in the governing equation, this parameter should be useful in many fields to study where particle trajectories are considered.

Acknowledgment

This work was supported in part by NASA Lewis Research Center under Grant NAG 3-28.

References

- ¹Ormsbee, A. I., Bragg, M. B., Maughmer, M. D., and Jordan, F. L., "Scaling Wake-Particle Interactions for Aerial Applications Research," *Journal of Aircraft*, Vol. 18, July 1981, pp. 592-596.
- ²Bragg, M. B., Gregorek, G. M., and Shaw, R. J., "An Analytical Approach to Airfoil Icing," AIAA Paper 81-0403, Jan. 1981.
- ³Ingelman-Sundberg, M., Trunov, O. K., and Ivaniko, A., "Methods for Prediction of the Influence of Ice on Aircraft Flying Characteristics," Joint Report from the Swedish-Soviet Working Group on Flight Safety, 6th Meeting, 1977.
- ⁴Langmuir, I. and Blodgett, K. B., "A Mathematical Investigation of Water Droplet Trajectories," Army Air Forces Tech. Rept. 5418, Contract W-33-038-ac-9151, Feb. 1946.
- ⁵Bowden, D. T., Gensemer, A. E., and Skeen, C. A., "Engineering Summary of Airframe Icing Technical Data," FAA, Washington, D. C., Tech Rept. ADS-4, March 1964.
- ⁶Sherman, P., Klein, J. S., and Tribus, M., "Determination of Drop Trajectories by Means of an Extension of Stokes Law," Project M992-D, Air Research and Development Command, United States Air Force Contract AF 18(600)-51, April 1952.
- ⁷Putnam, A., "Integratable Form of Droplet Drag Coefficient," *American Rocket Society Journal*, Vol. 31, Oct. 1961, pp. 1467-1468.
- ⁸Lozowski, E. P., Stallabrass, J. R., and Hearty, P. F., "The Icing of an Unheated Non-Rotating Cylinder in Liquid Water Droplet-Ice Crystal Clouds," National Research Council of Canada Div. of Mechanical Engineering, Rept. LTR-LT-96, Feb. 1979.
- ⁹Ormsbee, A. I. and Bragg, M. B., "Trajectory Scaling Laws for a Particle Injected into the Wake of an Aircraft," Univ. of Illinois, Aviation Research Laboratory, Rept. ARL-78-1, June 1978.
- ¹⁰Armand, C., Charpin, F., Fasso, G., and Leclerc, G., "Techniques and Facilities Used at the Onera Modane Centre for Icing Tests," AGARD Advisory Rept. 127, Nov. 1978, pp. A6-1-A6-23.
- ¹¹Haugher, H. H., Englar, K. G., and Reaser, W. W., "Analysis of Model Testing in an Icing Wind Tunnel," Douglas Aircraft Company, Inc., Rept. SM-14993, May 1954.
- ¹²Brun, R. J., Gallagher, H. M., and Vogt, D. E., "Impingement of Water Droplets on NACA 65A004 Airfoil and Effect of Change in Airfoil Thickness from 12 to 4 Percent at 4° Angle of Attack," NACA TN 3047, Nov. 1953.

From the AIAA Progress in Astronautics and Aeronautics Series . . .

VISCOUS FLOW DRAG REDUCTION—v. 72

Edited by Gary R. Hough, Vought Advanced Technology Center

One of the most important goals of modern fluid dynamics is the achievement of high speed flight with the least possible expenditure of fuel. Under today's conditions of high fuel costs, the emphasis on energy conservation and on fuel economy has become especially important in civil air transportation. An important path toward these goals lies in the direction of drag reduction, the theme of this book. Historically, the reduction of drag has been achieved by means of better understanding and better control of the boundary layer, including the separation region and the wake of the body. In recent years it has become apparent that, together with the fluid-mechanical approach, it is important to understand the physics of fluids at the smallest dimensions, in fact, at the molecular level. More and more, physicists are joining with fluid dynamicists in the quest for understanding of such phenomena as the origins of turbulence and the nature of fluid-surface interaction. In the field of underwater motion, this has led to extensive study of the role of high molecular weight additives in reducing skin friction and in controlling boundary layer transition, with beneficial effects on the drag of submerged bodies. This entire range of topics is covered by the papers in this volume, offering the aerodynamicist and the hydrodynamicist new basic knowledge of the phenomena to be mastered in order to reduce the drag of a vehicle.

456 pp., 6×9, illus., \$25.00 Mem., \$40.00 List

TO ORDER WRITE: Publications Dept., AIAA, 1290 Avenue of the Americas, New York, N.Y. 10104